Occlusal trauma accelerates attachment loss at the onset of experimental periodontitis in rats

Susumu Nakatsu (S.N.)[1,2], Yasunori Yoshinaga (Y.Y.)[1], Akiko Kuramoto (A.K.)[1], Fumiko Nagano (F.N.)[1], Ikuhisa Ichimura (I.I.)[2], Kazushi Oshino (K.O.)[2], Atsutoshi Yoshimura (A.Y.)[1], Yoshitaka Yano (Y.Y.)[2], Yoshitaka Hara (Y.H.)[1]

[1]Department of Periodontology, Nagasaki University Graduate School of Biomedical Sciences, Nagasaki, Japan

[2]Global R&D - Personal Health Care, Kao Corporation, Tokyo, Japan

Running title: Occlusal trauma and attachment loss

Corresponding author: Yoshitaka Hara, PhD, Department of Periodontology, Nagasaki University Graduate School of Biomedical Sciences, 1-7-1 Sakamoto, Nagasaki 852-8588, Japan; Tel: +81-95-819-7683; Fax: +81-95-819-7684; E-mail address: harasen@nagasaki-u.ac.jp

Key words: occlusal trauma, attachment loss, histopathological study, experimental periodontitis

Abstract

Background and objective: Occlusal trauma is an important factor that influences the progression of periodontitis, but it has been unclear whether occlusal trauma influences the periodontal destruction at the onset of periodontitis. We established an experimental periodontitis model with both site-specific loss of attachment and alveolar bone resorption. The purpose of the present study was to investigate the effects of occlusal trauma on periodontal destruction, particularly loss of attachment, at the onset of experimental periodontitis.

Materials and methods: Sixty rats were used in the present study. Forty-eight rats immunized with lipopolysaccharide (LPS) intraperitoneally were divided into four groups. In the T group, occlusal trauma was induced by placing an excessively high metal wire in the occlusal surface of the mandibular right first molar. In the I group, periodontal inflammation was induced by topical application of LPS into the palatal gingival sulcus of maxillary right first molars. In the T+I group, both trauma and periodontal inflammation were simultaneously induced. The PBS group was administered only phosphate buffered saline. Another non-immunized 12 rats (n-(T+I) group) were treated like as the T+I group. All rats were killed after 5 or 10 d, and their maxillary first molars with surrounding tissues were histopathologically observed. Loss

of attachment and osteoclasts on the alveolar bone crest were investigated histopathologically. To detect immune complexes, C1qB was immunohistologically stained. Collagen fibers were also observed with the picrosirius red-polarization method.

Results: There were significant increases in loss of attachment and the number of osteoclasts in the T+I group compared to the other groups. Moreover, widespread distribution of immune complexes was observed in the T+I group, and collagen fibers oriented from the root surface to the alveolar bone crest were partially disappeared in the T, T+I and n-(T+I) groups.

Conclusions: When inflammation was combined with occlusal trauma, immune complexes were confirmed in more expanding areas than in the area of the I group without occlusal trauma, and loss of attachment at the onset of experimental periodontitis was increased. Damage of collagen fibers by occlusal trauma may elevate the permeability of the antigen through the tissue and result in expanding the area of immune complex formation and accelerating inflammatory reaction. The periodontal tissue destruction was thus greater in the T+I group than in the I group.

Introduction

Occlusal trauma is generally regarded as an aggravating factor in periodontitis. Multiple studies have been conducted to elucidate the mechanisms underlying the important roles that occlusal trauma plays in periodontal pathology (1–5). Lindhe and Svanberg (1) and Ericsson and Lindhe (2) showed that angular bony defects and loss of attachment in dogs were influenced by the combined effect of plaque-induced periodontitis and jiggling-type trauma. In contrast, Meitner (4) and Polson et al. (5) reported that jiggling-type trauma in ligature-induced periodontitis does not influence the increase of loss of attachment. Furthermore, even if occlusal trauma truly influences periodontitis, the mechanism how it influences the periodontal destruction at the onset and progression of periodontitis is unclear.

We recently reported that alternate topical applications of lipopolysaccharide (LPS) and anti-LPS immunoglobulin G (IgG) into rat gingival sulcus induced loss of attachment, and, using anti-C1qB as a marker of immune complexes, we detected immune complexes in the junctional epithelium and adjacent connective tissue into which neutrophils were infiltrating (6). These findings strongly suggested that the formation of immune complex accelerates the loss of attachment by inducing an infiltration of neutrophils. In addition, we observed both site-specific loss of attachment

and alveolar bone resorption with the topical application of LPS into rat gingival sulcus when the serum level of anti-LPS IgG in rats was elevated after immunization with LPS (7). This model is well suited for investigations of periodontal destruction at the onset of periodontitis. The purpose of the present experimental study was to investigate the effects of occlusal trauma on the periodontal destruction at the onset of periodontitis, particularly loss of attachment.

Materials and Methods

Experimental Design

Forty-eight male nine-wk-old Lewis rats received intraperitoneal injections of 0.3 mL of 150 μg *Escherichia coli* (*E. coli*) LPS (O111: B4; Sigma, St. Louis, MO, USA) suspended in phosphate buffered saline (PBS) emulsified in complete Freund's adjuvant. Subsequently, these rats received a booster injection of LPS emulsified in incomplete Freund's adjuvant 28 days later (day 0: baseline) (8). Another 12 male nine-wk-old Lewis rats received intraperitoneal injections of 0.3 mL of PBS emulsified in complete Freund's adjuvant, followed by a booster injection of PBS emulsified in incomplete Freund's adjuvant 28 days later. According to the combination of experimental occlusal trauma and periodontitis, the 48 LPS-immunized rats were divided into four groups as follows: the trauma group (T group), the inflammation

group (I group), the trauma + inflammation group (T+I group), and the PBS group treated topically with PBS vehicle. Twelve other, non-immunized rats were designated as a non-immunized trauma + inflammation group (n-(T+I) group).

For excessive occlusal loading to the maxillary right first molar (9), the occlusal surface of the mandibular right first molar was raised by placing a metal wire (1.0 mm diameter) bonded with resin cements (Super-Bond C&B; Sun Medical, Shiga, Japan) as an occlusal interference under general anesthesia with sodium pentobarbital at 25 mg/kg of body weight at one day after the booster injection in the T group, the T+I group and the n-(T+I) group. For the induction of experimental periodontitis (7), the I group, the T+I group and the n-(T+I) group received daily topical applications of *E. coli* LPS in PBS (50 μg/μL) on the palatal gingival sulcus of the maxillary right first molar with a micropipette (under general anesthesia with isoflurane) just after the wire was placed on the mandibular first molar on the day after the booster injection. In total, 18 μL (3 μL, six times at intervals of 5 min) of LPS solution was topically administered daily. The T group and the PBS group received daily topical applications of only PBS in the same manner. The rats were killed under anesthesia with diethyl ether on days 5 and 10, 1 h after application of LPS or PBS.

All rats were purchased from Charles River Japan (Tokyo, Japan) and

maintained in specific pathogen-free conditions in the Biomedical Research Center, Center for Frontier Life Sciences (Nagasaki University, Nagasaki, Japan). Animal care and experimental procedures were performed in accordance with the Guidelines for Animal Experimentation of Nagasaki University and with the approval of the Institutional Animal Care and Use Committee.

Indirect ELISA for anti-LPS IgG detection

Blood samples were collected from the retro-orbital venous plexus of the rats at baseline, and immediately after the topical application of LPS or PBS on days 5 and 10. The levels of anti-LPS IgG in serum samples of individual rats were determined using an indirect ELISA. Microtiter plates with 96 wells were coated with 100 μL/well of a 2.5 μg/mL solution of LPS from *E. coli* in 0.05 M carbonate buffer (pH 9.6) and then incubated 16 h at 4ºC. After being washed with 0.05 % Tween20/PBS (PBST), the wells were blocked with 0.1 % bovine serum albumin (BSA)/PBS at room temperature. After another wash with PBST, 100 μL of the sera (1:1,000 dilutions) to be tested was added, and the plates were incubated for 1 h at room temperature. After a further washing with PBST, 100 μL of horseradish peroxidase (HRP)-conjugated goat anti-rat IgG (1:4,000 dilutions, Invitrogen, Tokyo, Japan) in PBS was added and incubated for

1 h at room temperature. The plates were washed with PBST, and 75 μL of the tetramethylbenzidine substrate solution (R&D Systems, Minneapolis, MN, USA) was added and incubated at room temperature. The enzyme reaction was stopped with 25 μL/well of 1 M H_2SO_4, and the absorbance was read at 450 nm on a microplate reader.

Preparation of tissue specimens

The maxillary right molar region was resected from each rat and fixed in 4% paraformaldehyde/PBS at 4ºC for 10 h. Subsequently, the specimens were decalcified by immersion in 10% EDTA-2Na (pH 7.4) at 4ºC for 3 wks and then embedded in paraffin by the AMeX method (10). Briefly, the specimens were dehydrated in acetone, consecutively, cleared in methyl benzoate for 30 min and in xylene for 30 min, and then penetrated with paraffin at 60°C for 2 h. The penetrated specimens were then embedded into paraffin blocks. Paraffin-embedded buccopalatal serial sections (4-μm thickness) were obtained.

Histopathological, histometrical and immunohistological analyses

Five groups of serial sections, each containing 10 subsections, were obtained

from each specimen. The first subsections from each group of serial sections were stained with hematoxylin and eosin for histopathological observation. These sections were used for the histometrical analysis using image analysis software (ImageJ; National Institutes of Health, Bethesda, MD, USA). The distance between the cemento-enamel junction (CEJ) and the coronal position of the junctional epithelium attached to the root surface (Fig. 1) was measured as the loss of attachment.

The second subsections from each group of serial sections were stained with TRAP according to the procedure described by Katayama et al. (11) to identify osteoclasts. Briefly, a staining solution was made by mixing 0.5 mL of pararosaniline solution (1.0 g of pararosaniline/20 mL of distilled water + 5 mL of concentrated HCl), 0.5 mL of 4% sodium nitrite solution, 10 mL of 0.1 M acetate buffer (pH 5.0), and 8 mL of 0.125 % naphthol AS-BI phosphate (Sigma) solution. The mixture was adjusted to pH 5.0 using NaOH and filtered through Whatman grade no. 1 filter paper. Then, 150 mg of L-(+)-tartaric acid was added to a 10-mL aliquot of the solution. After the sections from each group had been incubated in the staining solution for 30 min at 37ºC, they were counterstained with Mayer's hematoxylin. The numbers of TRAP-positive multinuclear cells in an area of 500-μm width on the surface of the alveolar bone were counted (Fig. 1).

In general, to observe immune complex immunohistologically, antigen and antibody are investigated individually. But in our serial studies (6, 7, 12), it was difficult to detect localization of antigens and their specific antibodies immunohistologically. When the activation of the classical pathway of complement is initiated, the C1 component binds to antigen-bound antibodies. Therefore, we used immunohistological detection of C1qB to identify the location of immune complexes in rat gingiva. Then in the present study, the third subsections from each group of serial sections were used for the immunohistological staining of C1qB as described (6). Briefly, after the sections were deparaffinized, endogenous peroxidase activity was blocked with 0.3% H_2O_2/methanol for 30 min, followed by incubation in normal goat serum at room temperature for 30 min. These sections were then immersed in rabbit polyclonal anti-C1qB (Aviva Systems Biology, San Diego, CA, USA) at 4ºC for 16 h. Sections were then incubated with biotinylated goat anti-rabbit polyclonal immunoglobulin (Dako, Glostrup, Denmark) at room temperature for 30 min, after which the sections were incubated with peroxidase-conjugated streptavidin (Dako) at room temperature for 30 min. Finally, sections were incubated with diaminobenzidine tetraoxide solution and counterstained with Mayer's hematoxylin. The area where immune complexes were stained immunohistologically was quantified in the sections in I group and T+I group

using a light microscope with a microscopic grid of 100 squares in an area of 0.25 mm^2 at ×400 magnification. The positively stained area was determined by counting the grids.

The fourth subsections from each group of serial sections were used for the picrosirius red staining (Picrosirius red stain kit; Polysciences, Warrington, PA, USA) to observe collagen fibers. Briefly, the sections were deparaffinized and then stained with Weigert's iron hematoxylin for 8 min. After washing with distilled water, the sections were immersed in phosphomolybdic acid hydrate solution for 2 min. The sections were stained with picrosirius red F3BA solution for 110 min, and then washed with 0.01 N HCl. The sections stained with picrosirius red were observed by polarizing microscope (ECLIPSE LV100POL; Nikon, Tokyo, Japan). In the polarizing microscope under crossed nicols, the polarization color and the orientation of collagen fibers in the sections were investigated.

Statistical analysis

The data were analyzed using the STATMATE software program (Abacus Concepts, Berkeley, CA, USA). Differences among the five groups were assessed using a one-factor ANOVA and the Tukey-Kramer test. Differences between the I group and

the T+I group were assessed using the Mann-Whitney U-test. A value of $p<0.05$ was considered significant. The values are expressed as means ± SD.

Results

The serum level of anti-LPS IgG

The serum levels of anti-LPS IgG were elevated in all four LPS-immunized groups throughout the experimental period. No significant differences were observed in the anti-LPS IgG levels among the LPS-immunized groups. In contrast, the serum level of anti-LPS IgG was quite low in the n-(T+I) group. The serum levels of anti-LPS IgG in the LPS-immunized groups were significantly higher than that in n-(T+I) group at all time points ($p<0.01$).

Histopathological findings

The furcation area showed hyaline degeneration and irregular bone surface with appearance of osteoclasts on day 5 in the T, T+I, and n-(T+I) groups. Slight hyaline degeneration of periodontal tissue and no irregular bone surface were observed in the furcation area on day 10 (data not shown).

Day 5:

In the PBS group and the T group, slight infiltrations of inflammatory cells were observed in the junctional epithelium and adjacent connective tissue, whereas apical migration of the junctional epithelium and loss of attachment were not observed (Fig. 2A). In the I group, inflammatory cells, mainly neutrophils, infiltrated the junctional epithelium and adjacent connective tissue, and the junctional epithelium migrated apically (Fig. 2B). Slight loss of attachment was observed on the palatal side of the gingiva where LPS was applied in 2 blocks/6 blocks in the I group. The T+I group showed inflammatory cell infiltration in the junctional epithelium and adjacent connective tissue and loss of attachment in all six blocks (Fig. 2C). In the n-(T+I) group, loss of attachment was not detected, and slight apical migration of the junctional epithelium was observed in some of the specimens (Fig. 2D). Inflammatory cell infiltration in the n-(T+I) group was increased compared with the PBS and T groups.

Day 10:

In the PBS and T groups, slight infiltration of inflammatory cells was observed in the junctional epithelium and adjacent connective tissue, and neither apical migration of the junctional epithelium nor loss of attachment were observed. The I group showed inflammatory cell infiltration, mainly neutrophils, in the junctional epithelium and adjacent connective tissue and loss of attachment in all six blocks (Fig. 3A). The T+I

group also showed similar inflammatory cell infiltration and loss of attachment (Fig. 3B). Irregular palatal alveolar bone surfaces were observed only in the T+I group. Loss of attachment was not detected and slight apical migration of junctional epithelium was observed in the n-(T+I) group (Fig. 3C). Inflammatory cell infiltration in the n-(T+I) group increased compared with the PBS and T groups.

Histometrical analysis of loss of attachment

No loss of attachment was observed in the PBS group, the T group or the n-(T+I) group. The I group on day 5 and day 10 exhibited an average of 28.4 ± 39.6 μm and 139.9 ± 42.9 μm of loss of attachment, respectively. The T+I group on day 5 and day 10 exhibited an average of 170.6 ± 17.7 μm and 237.8 ± 25.3 μm loss of attachment, respectively. Loss of attachment was significantly deeper in the T+I group than in the I group on day 5 and day 10 ($p<0.001$; Fig. 4A, B).

Histometrical analysis of TRAP-positive osteoclasts

TRAP-positive cells were not observed on the palatal alveolar bone crest in the PBS group, the T group or the n-(T+I) group. A few TRAP-positive cells at the edge of the palatal alveolar bone were seen in the I group on day 5 and day 10 (Fig. 5A). The

numbers of TRAP-positive cells on day 5 and day 10 were an average of 0.33 ± 0.72 cells/unit and 0.43 ± 0.51 cells/unit, respectively. The T+I group showed many TRAP-positive cells on alveolar bone crest on day 10, although only a few TRAP-positive cells were seen on day 5 (Fig. 5B). The numbers of TRAP-positive cells on day 5 and day 10 showed an average of 0.43 ± 0.34 cells/unit and 7.73 ± 2.81 cells/unit, respectively. There was a significantly higher number of TRAP-positive cells in the T+I group on day 10 than in the other groups ($p<0.001$), although no significant differences in this parameter were observed among the five groups on day 5 (Fig. 5C, D).

Immunohistological findings of C1qB

C1qB in the PBS group, the T group and the n-(T+I) group was not detected on days 5 or 10. C1qB in the I group on day 5 was localized in the junctional epithelium and adjacent connective tissue where inflammatory cells were infiltrating (Fig. 6A). C1qB in the T+I group was more widely observed within the junctional epithelium and adjacent connective tissue on day 5 (Fig. 6B, C). The location of C1qB in the I and T+I groups on day 10 was similar to that in the T+I group on day 5.

Polarizing microscopic findings

Under the polarizing microscope, yellow and green collagen fibers oriented from the root surface towards the alveolar bone crest were observed in the PBS and the I group on day 5 (Fig. 7A, B). The yellow fibers towards the alveolar bone crest were partially decreased or absent in the T group, T+I group and n-(T+I) group on day 5 (Fig. 7C, D). These changes of collagen fibers were still observed on day 10.

Discussion

In the present study, loss of attachment was observed only in the I and T+I group; the T and the n-(T+I) groups showed no loss of attachment. In the I group and the T+I group, C1qB was detected in the junctional epithelium and adjacent connective tissue, and inflammatory cells (predominantly neutrophils) infiltrated the junctional epithelium and adjacent connective tissue. These findings suggest that LPS and the anti-LPS IgG in the serum and the gingival crevicular fluid formed immune complexes, and these immune complexes then accelerated inflammatory cell infiltration. Yoshinaga et al. (7) also observed both the immunolocalization of C1qB in the same region and loss of attachment. Moreover, loss of attachment was not observed in the present study's n-(T+I) group. This result strongly suggested that loss of attachment required an

antigen-antibody reaction and subsequent neutrophils infiltration. A 2012 report showed that aging-associated periodontitis is accompanied by a lower expression of Del-1, an endogenous inhibitor of neutrophil adhesion (13). Thus, infiltrating neutrophils are thought to have a major effect on the tissue destruction and progression of periodontitis.

Although many relevant animal experiments have been performed, little is known about the effects of occlusal trauma on periodontal inflammation. Glickman (14) proposed the co-destructive theory in which excessive trauma alters the pathway of inflammation. Lindhe et al. (1, 2) have reported that trauma such as jiggling force aggravates irreversible loss of periodontal supportive tissues in advanced periodontitis. In contrast, Waerhaug (15) reported that there is no relationship between occlusal trauma and the degree of angular bony defects and infrabony pocket. In the present study C1qB was widespread and greater loss of attachment was observed in the T+I group compared to the I group. Thus, we consider that the spread of immune complexes may be an important factor in the mechanism underlying how occlusal trauma accelerates the loss of attachment. Neiderud et al. (16) and Biancu et al. (17) observed a reduced amount of supra-alveolar collagen in a model of jiggling traumatic occlusion, and they suggested that the alterations of the supra-alveolar tissue could influence the route of spread of inflammation. In the present study, we showed that collagen fibers

oriented from the root surface towards alveolar bone crest decreased or disappeared. These results suggested that the destruction of collagen fibers might increase the permeability of the antigen. In the T+I group, spreading antigens made the area of forming immune complex wider, and then the inflammatory cell infiltration and tissue destruction became stronger.

Glickman (14) and Lindhe et al. (1, 2) have investigated the influence of traumatic occlusion in advanced stages of periodontitis. Our findings, especially bone resorption, were different from their findings. However, the purpose of the present study was to investigate the early stage of periodontitis with traumatic occlusion. Thus, we did not demonstrate the alteration of the direction of the collagen fibers when the periodontal destruction had advanced. If the collagen fiber direction in the advanced stage of this experimental periodontitis is the same as their experiments, the pathological condition would also be the same as theirs. If the different direction of occlusal force caused different areas of collagen destruction, the route of the antigen spreading would also be different. This change might influence on the shape of bone defect. Further studies are necessary to elucidate this point.

Methods to induce experimental occlusal trauma by bonding an excessive-height inlay on rodent molar have been reported (9, 18–21). These models are well suited for

investigations of periodontal breakdown, but the traumatic forces in these models gradually decrease (22). In our preliminary experiment, degeneration and bone resorption were not observed 15 days after the placement of a metal wire, and the excessive traumatic force had not been maintained (data not shown). Thus, the present experimental period was limited to 10 days, a period in which the traumatic force was maintained. In our study, the trauma groups exhibited the hyaline degeneration of periodontal ligament tissue and alveolar bone resorption in the furcation area with appearance of osteoclast like cells. These findings correspond precisely to our earlier study (9).

Several studies showed that the antigen could penetrate the junctional epithelium from the gingival sulcus to the gingival connective tissue. Topically applied horseradish peroxidase (HRP) penetrates the junctional epithelium to the periodontal tissue (23, 24) and regional lymph nodes (25). We attempted to clarify the change of ground substance of connective tissue with histochemical staining of hyaluronan using biotinylated hyaluronan binding protein and alcian blue staining; however, we could not find any marked difference in the ground substance depending on the presence or absence of occlusal trauma (data not shown). Moreover, a 2006 report (26) showed that activation of a putative mechanosensitive channel changes epithelial permeability. In addition, a

mechanical tugging force regulates the size of cell-cell junctions in endothelial cells (27). Thus, it is possible that the excessive occlusal force enhanced the permeability of the antigen through the junctional epithelium, and/or unknown changes of ground substance led to the widespread immune complex formation observed in the present study.

More TRAP-positive cells at the alveolar bone crest were seen in the T+I group than in the I group on day 10. Occlusal trauma surely accelerated the LPS-induced bone resorption. RANKL is an important factor in osteoclast formation (28–31). Moreover, LPS (32) and complement C3a and C5a (33) produced by the classical pathway of complement activation directly stimulate osteoclast formation. Although we did not immunohistochemically observe immune complexes in the bone resorption area in the present study, LPS and/or activated complements might be related to osteoclast formation. Further, bone-resorbing cytokines (such as interleukin-1 and tumor necrosis factor-alpha) produced by inflammatory cells induce RANKL expression (34, 35), and then neutrophils infiltrating to the inflamed site might produce tumor necrosis factor-alpha and RANKL (36) and contribute to osteoclast differentiation.

In conclusion, occlusal trauma by itself did not result in loss of attachment, but it accelerated periodontal tissue destruction, loss of attachment and bone resorption when

it was combined with inflammation. Occlusal trauma caused the degeneration of collagen fibers and probably increased the permeability of antigens. The immune complex then spread widely, and the infiltration of inflammatory cells, which is related to tissue destruction, became stronger.

Acknowledgements

We thank Dr. T. Shiraishi of Nagasaki University for the polarizing microscopic analysis and the staff of the Biomedical Research Center, Center for Frontier Life Sciences, Nagasaki University, for their maintenance of the experimental animals. This study was supported by grants (24593127 and 24890169) for scientific research from the Ministry of Education, Culture, Sports, Science and Technology of Japan.

References

1. Lindhe J, Svanberg G. Influence of trauma from occlusion on progression of experimental periodontitis in the beagle dog. *J Clin Periodontol* 1974; **1**: 3–14.
2. Ericsson I, Lindhe J. Effect of longstanding jiggling on experimental marginal periodontitis in the beagle dog. *J Clin Periodontol* 1982; **9**: 497–503.
3. Nyman S, Lindhe J, Ericsson I. The effect of progressive tooth mobility on destructive periodontitis in the dog. *J Clin Periodontol* 1978; **5**: 213–225.
4. Meitner S. Co-destructive factors of marginal periodontitis and repetitive mechanical injury. *J Dent Res* 1975; **54**: C78–C85.
5. Polson AM, Zander HA. Effect of periodontal trauma upon intrabony pockets. *J Periodontol* 1983; **54**: 586–591.
6. Kuramoto A, Yoshinaga Y, Kaneko T, et al. The formation of immune complexes is involved in the acute phase of periodontal destruction in rats. *J Periodontal Res* 2012; **47**: 455–462.
7. Yoshinaga Y, Ukai T, Kaneko T, et al. Topical application of lipopolysaccharide into gingival sulcus promotes periodontal destruction in rats immunized with lipopolysaccharide. *J Periodontal Res* 2012; **47**: 674–680.
8. Gor DO, Ding X, Li Q, Schreiber JR, Dubinsky M, Greenspan NS. Enhanced

immunogenicity of pneumococcal surface adhesin A by genetic fusion to cytokines and evaluation of protective immunity in mice. *Infect Immun* 2002; **70**: 5589–5595.

9. Yoshinaga Y, Ukai T, Abe Y, Hara Y. Expression of receptor activator of nuclear factor kappa B ligand relates to inflammatory bone resorption, with or without occlusal trauma, in rats. *J Periodontal Res* 2007; **42**: 402–409.
10. Sato Y, Mukai K, Watanabe S, Goto M, Shimosato Y. The AMeX method. A simplified technique of tissue processing and paraffin embedding with improved preservation of antigens for immunostaining. *Am J Pathol* 1986; **125**: 431–435.
11. Katayama I, Li CY, Yam LT. Histochemical study of acid phosphatase isoenzyme in leukemic reticuloendotheliosis. *Cancer* 1972; **29**: 157–164.
12. Nagano F, Kaneko T, Yoshinaga Y, et al. Gram-positive bacteria as an antigen topically applied into gingival sulcus of immunized rat accelerates periodontal destruction. *J Periodontal Res* 2013; **48**: 420–427.
13. Eskan MA, Jotwani R, Abe T, et al. The leukocyte integrin antagonist Del-1 inhibits IL-17-mediated inflammatory bone loss. *Nat Immunol* 2012; **13**: 465–473.
14. Glickman I. Occlusion and the periodontium. *J Dent Res* 1967; **46**: 53–59.
15. Waerhaug J. The infrabony pocket and its relationship to trauma from occlusion and subgingival plaque. *J Periodontol* 1979; **50**: 355–365.

16. Neiderud AM, Ericsson I, Lindhe J. Probing pocket depth at mobile/nonmobile teeth. *J Clin Periodontol* 1992; **19**: 754–759.

17. Biancu S, Ericsson I, Lindhe J. Periodontal ligament tissue reactions to trauma and gingival inflammation. An experimental study in the beagle dog. *J Clin Periodontol* 1995; **22**: 772–779.

18. Walker CG, Ito Y, Dangaria S, Luan X, Diekwisch TG. RANKL, osteopontin, and osteoclast homeostasis in a hyperocclusion mouse model. *Eur J Oral Sci* 2008; **116**: 312–318.

19. Kaku M, Uoshima K, Yamashita Y, Miura H. Investigation of periodontal ligament reaction upon excessive occlusal load - osteopontin induction among periodontal ligament cells. *J Periodontal Res* 2005; **40**: 59–66.

20. Goto KT, Kajiya H, Nemoto T, et al. Hyperocclusion stimulates osteoclastogenesis via CCL2 expression. *J Dent Res* 2011; **90**: 793–798.

21. Wan HY, Sun HQ, Sun GX, Li X, Shang ZZ. The early phase response of rat alveolar bone to traumatic occlusion. *Arch Oral Biol* 2012; **57**: 737–743.

22. Kenney EB. A histopathologic study of incisal dysfunction and gingival inflammation in the rhesus monkey. *J Periodontol* 1971; **42**: 3–7.

23. McDougall WA. Penetration pathways of a topically applied foreign protein into rat

gingiva. *J Periodontal Res* 1971; **6**: 89–99.

24. Romanowski AW, Squier CA, Lesch CA. Permeability of rodent junctional epithelium to exogenous protein. *J Periodontal Res* 1988; **23**: 81–86.

25. Abe T, Hara Y, Aono M. Penetration, clearance and retention of antigen en route from the gingival sulcus to the draining lymph node of rats. *J Periodontal Res* 1991; **26**: 429–439.

26. Reiter B, Kraft R, Günzel D, et al. TRPV4-mediated regulation of epithelial permeability. *FASEB J* 2006; **20**: 1802–1812.

27. Liu Z, Tan JL, Cohen DM, et al. Mechanical tugging force regulates the size of cell-cell junctions. *Proc Natl Acad Sci USA* 2010; **107**: 9944–9949.

28. Yasuda H, Shima N, Nakagawa N, et al. Osteoclast differentiation factor is a ligand for osteoprotegerin/osteoclastogenesis-inhibitory factor and is identical to TRANCE/RANKL. *Proc Natl Acad Sci USA* 1998; **95**: 3597–3602.

29. Suda T, Takahashi N, Udagawa N, Jimi E, Gillespie MT, Martin TJ. Modulation of osteoclast differentiation and function by the new members of the tumor necrosis factor receptor and ligand families. *Endocr Rev* 1999; **20**: 345–357.

30. Kong YY, Feige U, Sarosi I, et al. Activated T cells regulate bone loss and joint destruction in adjuvant arthritis through osteoprotegerin ligand. *Nature* 1999; **402**:

304–309.

31. Sato K, Suematsu A, Okamoto K, et al. Th17 functions as an osteoclastogenic helper T cell subset that links T cell activation and bone destruction. *J Exp Med* 2006; **203**: 2673–2682.

32. Kikuchi T, Matsuguchi T, Tsuboi N, et al. Gene expression of osteoclast differentiation factor is induced by lipopolysaccharide in mouse osteoblasts via Toll-like receptors. *J Immunol* 2001; **166**: 3574–3579.

33. Ignatius A, Schoengraf P, Kreja L, et al. Complement C3a and C5a modulate osteoclast formation and inflammatory response of osteoblasts in synergism with IL-1β. *J Cell Biochem* 2011; **112**: 2594–2605.

34. Jimi E, Nakamura I, Duong LT, et al. Interleukin 1 induces multinucleation and bone-resorbing activity of osteoclasts in the absence of osteoblasts/stromal cells. *Exp Cell Res* 1999; **247**: 84–93.

35. Hofbauer LC, Lacey DL, Dunstan CR, Spelsberg TC, Riggs BL, Khosla S. Interleukin-1β and tumor necrosis factor-α, but not interleukin-6, stimulate osteoprotegerin ligand gene expression in human osteoblastic cells. *Bone* 1999; **25**: 255–259.

36. Chakravarti A, Raquil MA, Tessier P, Poubelle PE. Surface RANKL of Toll-like

receptor 4-stimulated human neutrophils activates osteoclastic bone resorption. *Blood* 2009; **114**: 1633–1644.

Figure Legends

Fig. 1. Schema of rat periodontal tissue for histometrical analysis. Loss of attachment (X) was calculated by measuring the distance between the cemento–enamel junction (CEJ) and the coronal position of the junctional epithelium. TRAP-positive multinuclear cells were counted in an area of 500 lm width on the surface of the alveolar bone crest.

Fig. 2. Histopathological findings of loss of attachment on day 5. Hematoxylin and eosin (H&E) staining of the specimens from the PBS group (A), I group (B), T+I group (C) and n-(T+I) group (D) is shown. Both the I group and T+I group show loss of attachment. Loss of attachment in the T+I group is greater than in the I group (B, C). Black arrows indicate the cemento-enamel junction (CEJ). White arrows indicate the coronal position of the junctional epithelium . Scale bars = 100 μm.

Fig. 3. Histopathological findings of loss of attachment on day 10. H&E staining of the specimens from the I group (A), T+I group (B) and n-(T+I) group (C) is shown. Loss of attachment is observed in both the I group and T+I group but not in the n-(T+I) group. Loss of attachment in the T+I group is greater than in the I group. Black arrows indicate the CEJ. White arrows indicate the coronal position of the junctional epithelium. Scale

bars = 100 μm.

Fig. 4. Histometrical analysis of loss of attachment. The distance from the CEJ to the coronal position of the junctional epithelium attachment was analyzed histometrically as loss of attachment on day 5 (A) and day 10 (B). The PBS group, T group and n-(T+I) group showed no loss of attachment on day 5 or day 10. Loss of attachment is significantly greater in the T+I group than in the I group on day 5 and day 10. Each symbol = mean ± SD. *$p<0.001$.

Fig. 5. Histopathological findings of TRAP staining and the number of TRAP-positive cells. A few osteoclasts are located on the bone surface in the I group on day 10 (A, arrowheads). The alveolar bone surface remains smooth. Many osteoclasts are observed on the irregular bone surface in the T+I group on day 10 (B, arrowheads). There is no significant difference among five groups on day 5 (C). The number of TRAP-positive cells in the T+I group on day 10 is significantly greater than the other groups (D). Each bar = mean + SD. *$p<0.001$. ABC: alveolar bone crest. Scale bars = 50 μm.

Fig. 6. Immunohistochemical localization of C1qB. C1qB (stained dark red) is localized

in the junctional epithelium and adjacent connective tissue of the I group on day 5 (A). The presence of C1qB is widely distributed in the junctional epithelium and adjacent connective tissue of the T+I group on day 5 (B). Quantitative assessment of the area where immune complexes were stained immunohistologically in the sections in I group and T+I group on day 5 (C). Mann-Whitney U-test, *P<0.01. Scale bars = 100 μm.

Fig. 7. Polarizing microscopic findings of picrosirius red-stained section. Collagen fibers oriented from the root surface towards the alveolar bone crest show a high prevalence of yellow polarization color in the PBS group on day 5 (A and B, circled area). The yellow fibers were partially disappeared in the T group on day 5 (C and D, circled area). B and D show micrographs with the crossed polars rotated 45 degrees to the original micrographs (A and C, respectively). R: root. ABC: alveolar bone crest. Scale bars = 100 μm.

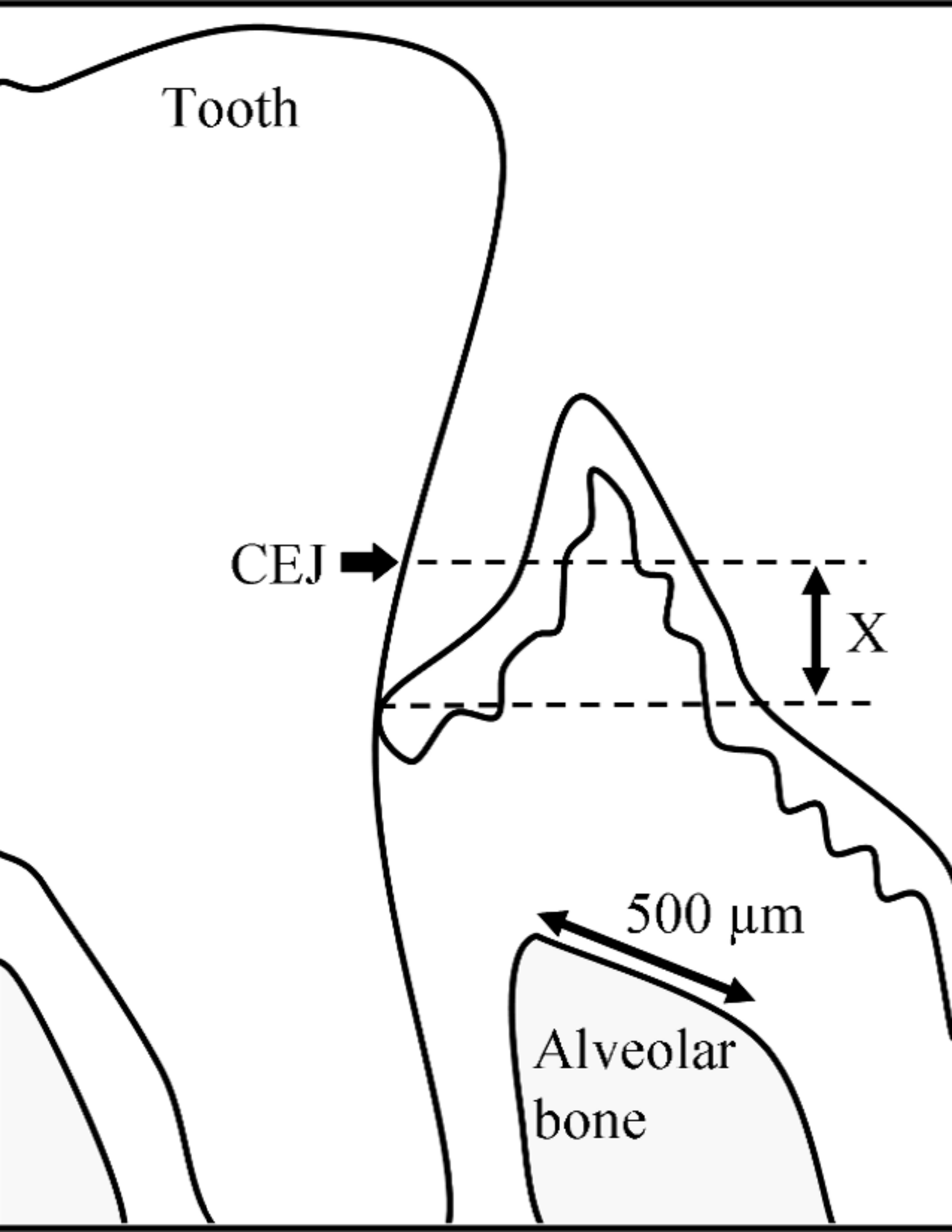
Tooth
CEJ
X
500 µm
Alveolar
bone

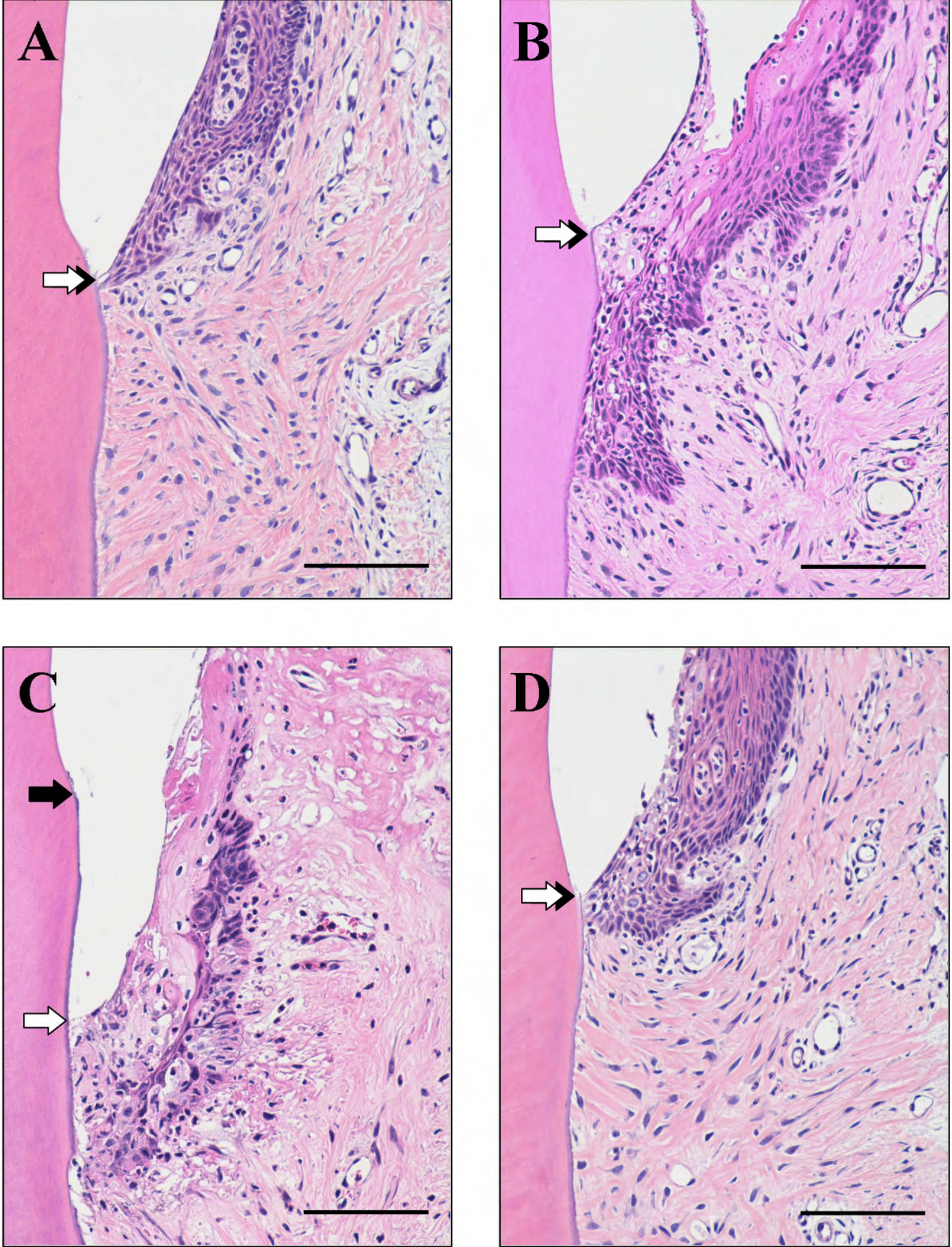
A
B
C
D

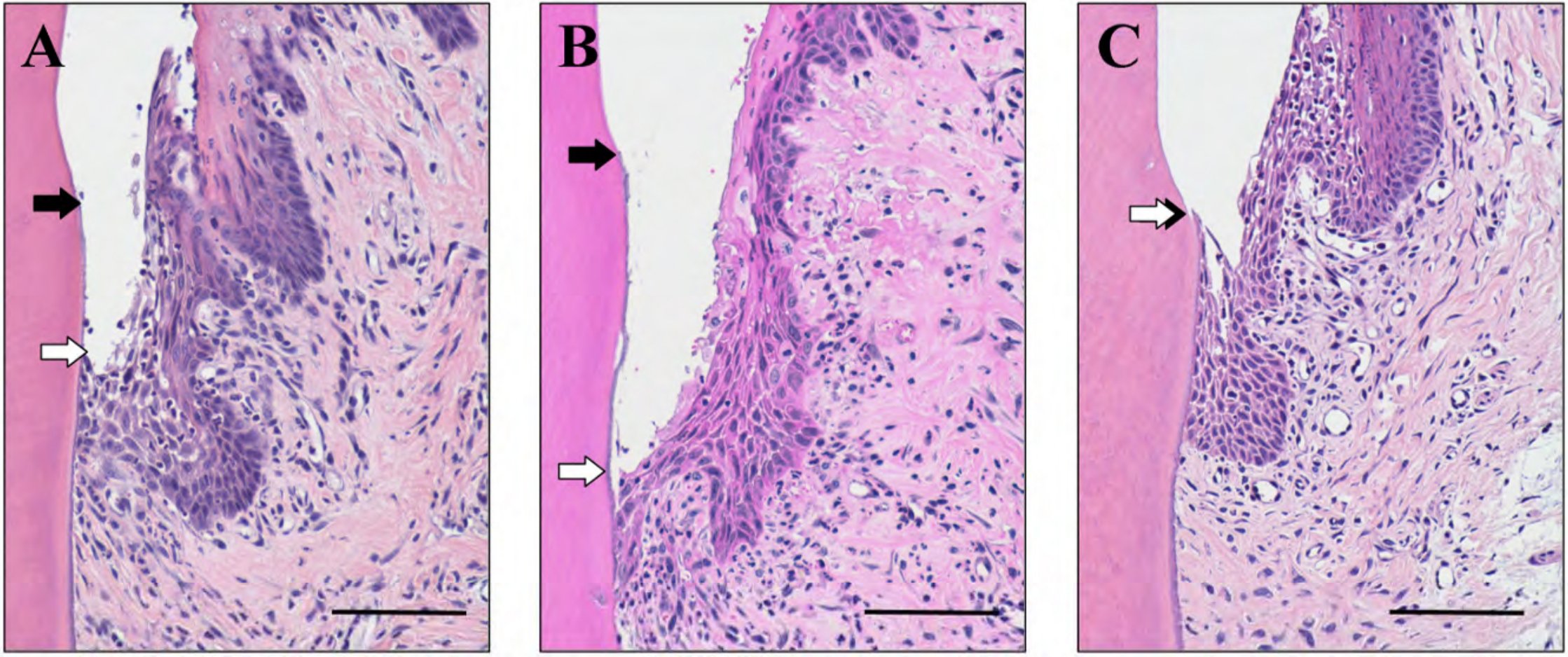
A
B
C

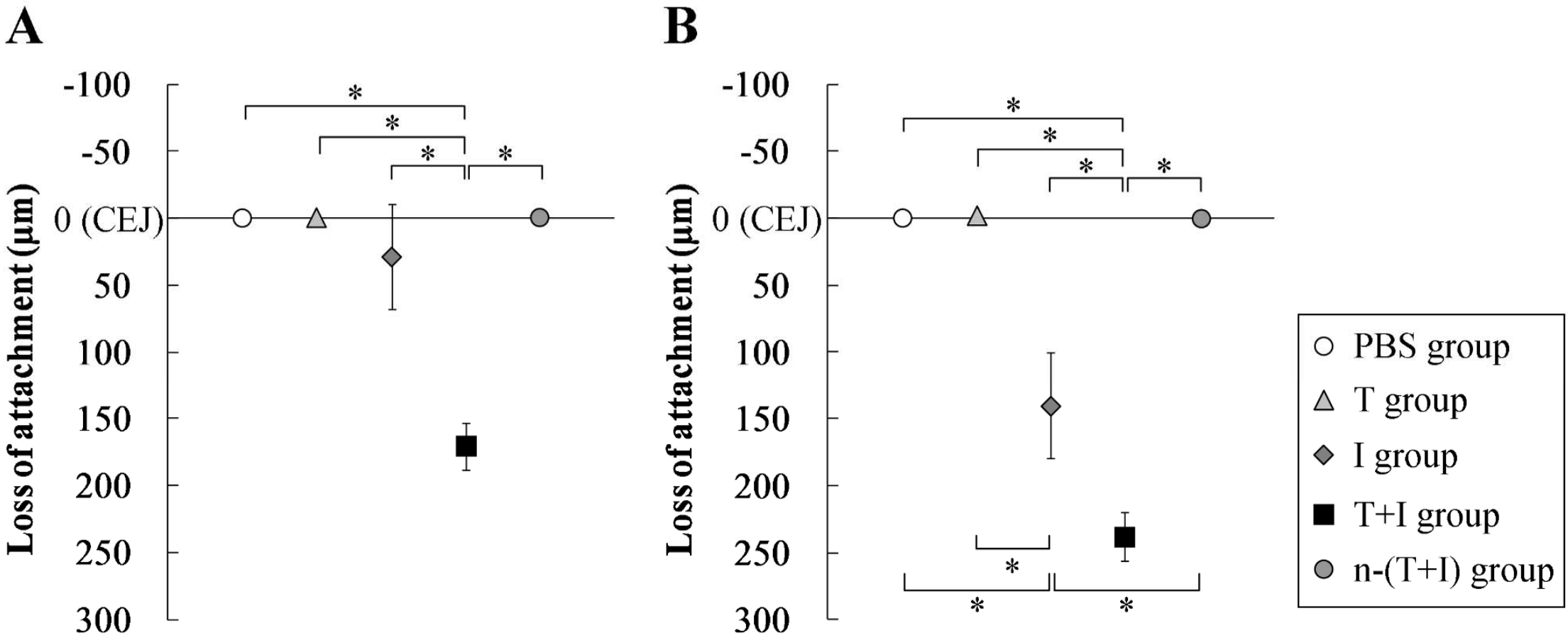
A
B
-100
-50
0 (CEJ)
50
100
150
200
250
300
Loss of attachment (μm)
*
PBS group
T group
I group
T+I group
n-(T+I) group

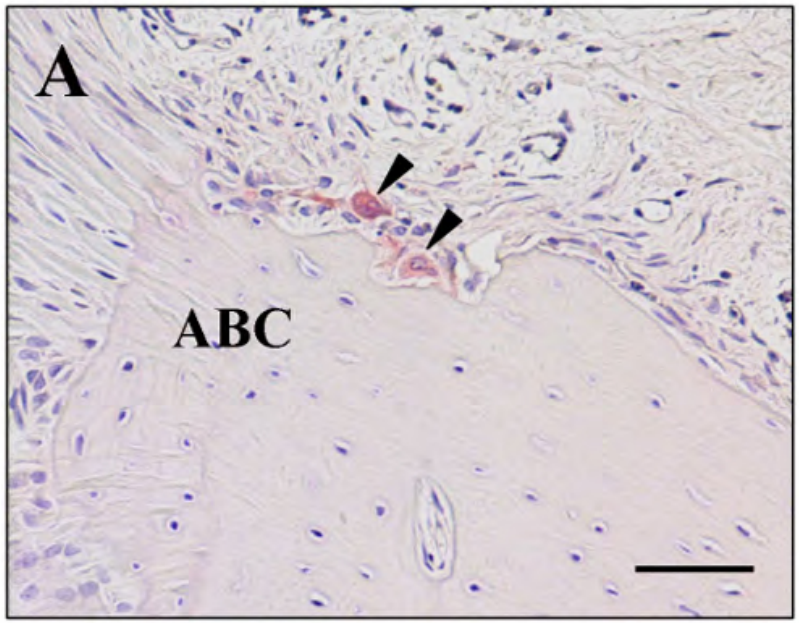
A
ABC

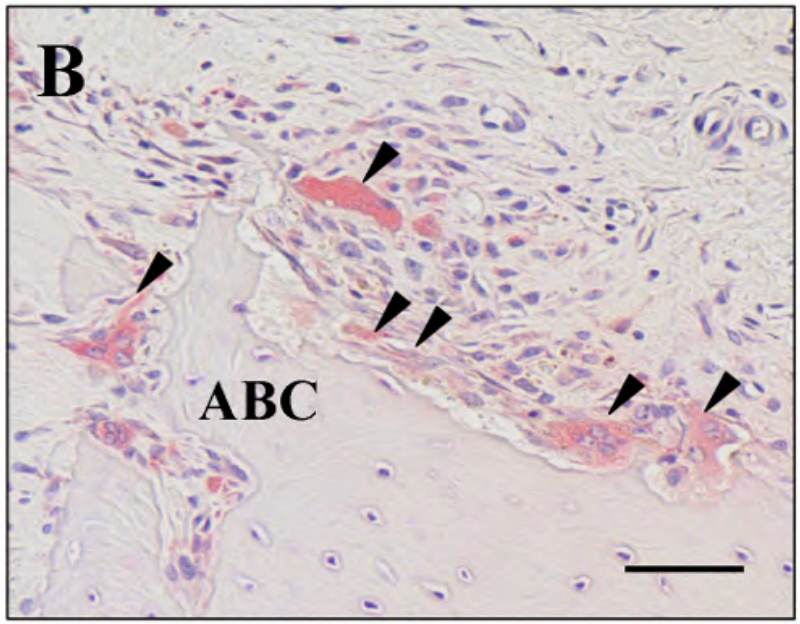
B
ABC

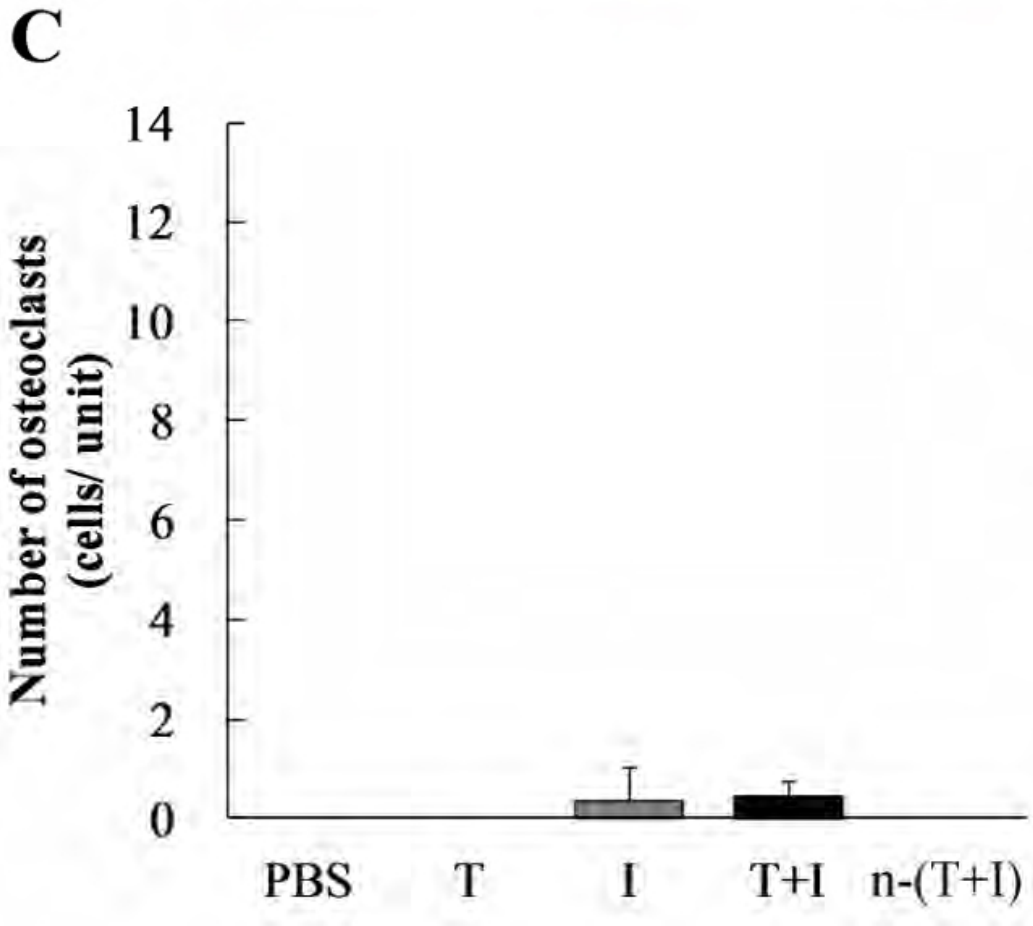
C
Number of osteoclasts (cells/ unit)
14
12
10
8
6
4
2
0
PBS
T
I
T+I
n-(T+I)

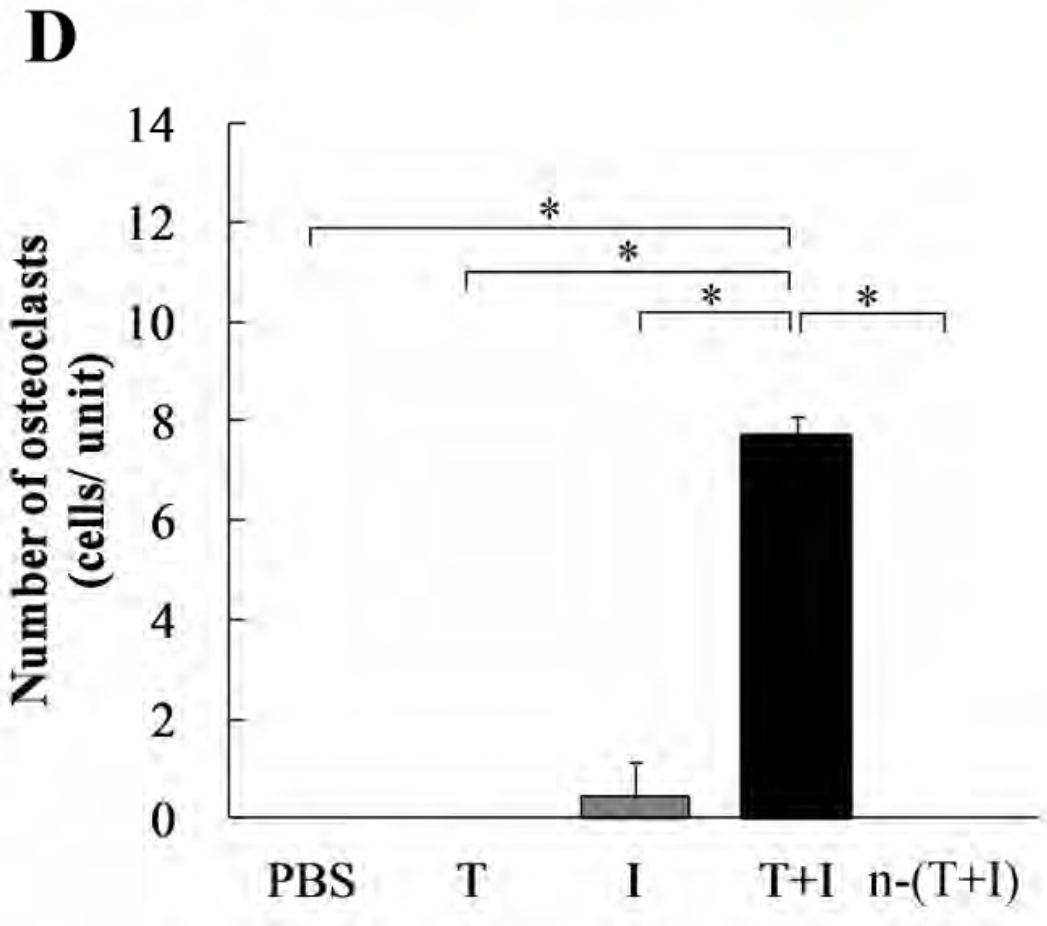
D
Number of osteoclasts (cells/ unit)
14
12
10
8
6
4
2
0
*
*
*
*
PBS
T
I
T+I
n-(T+I)

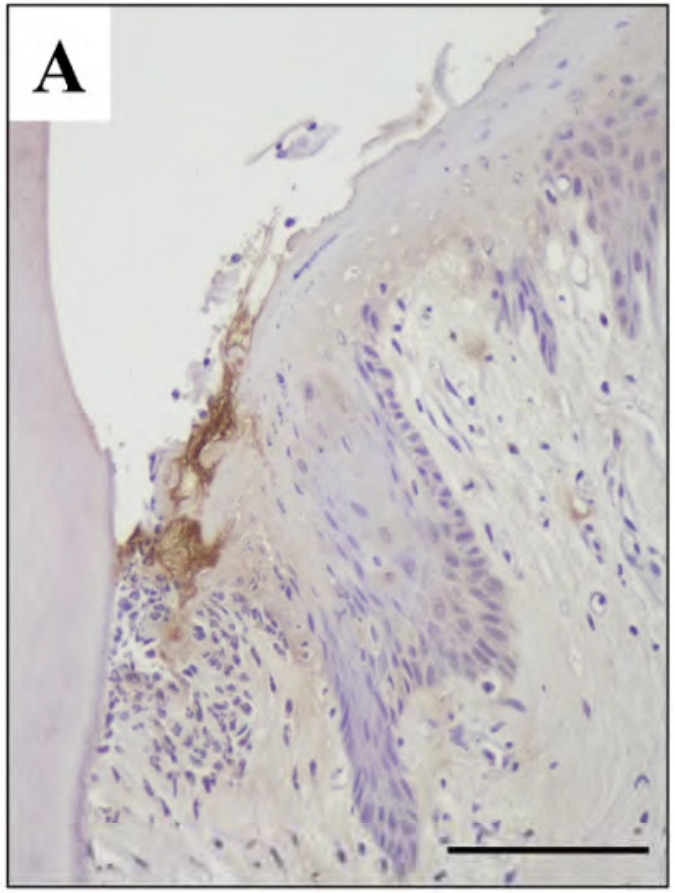
A

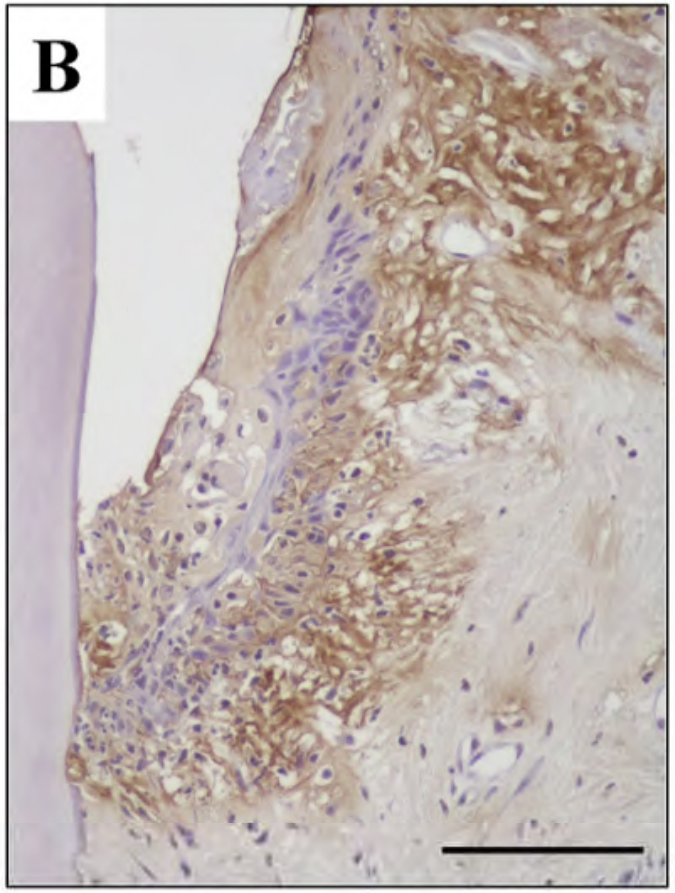
B

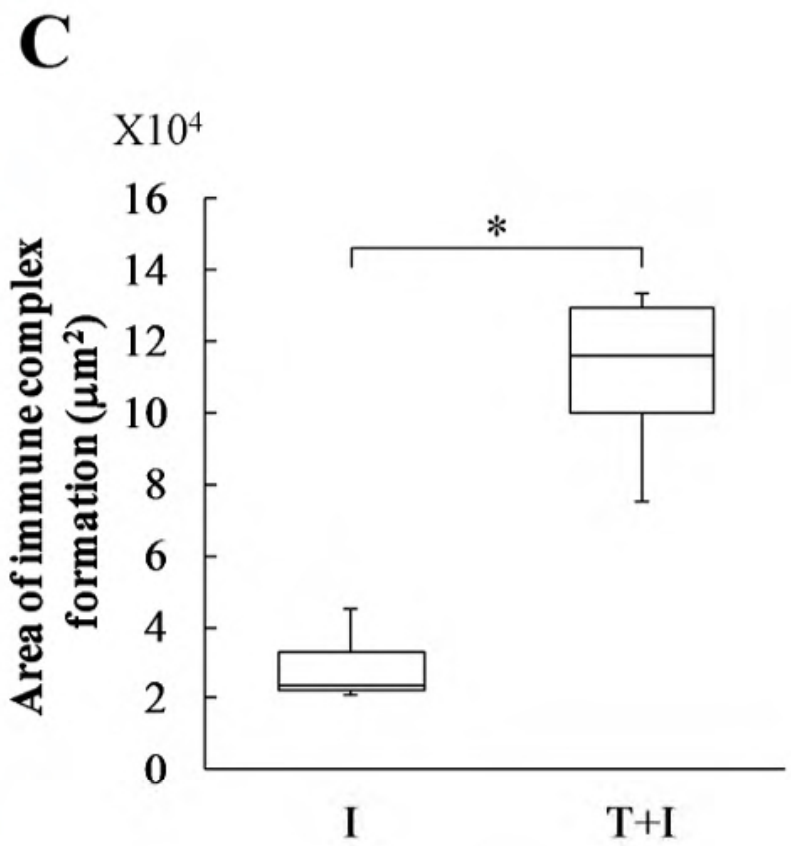
C
X10⁴
16
14
12
10
8
6
4
2
0
Area of immune complex formation (μm²)
*
I
T+I

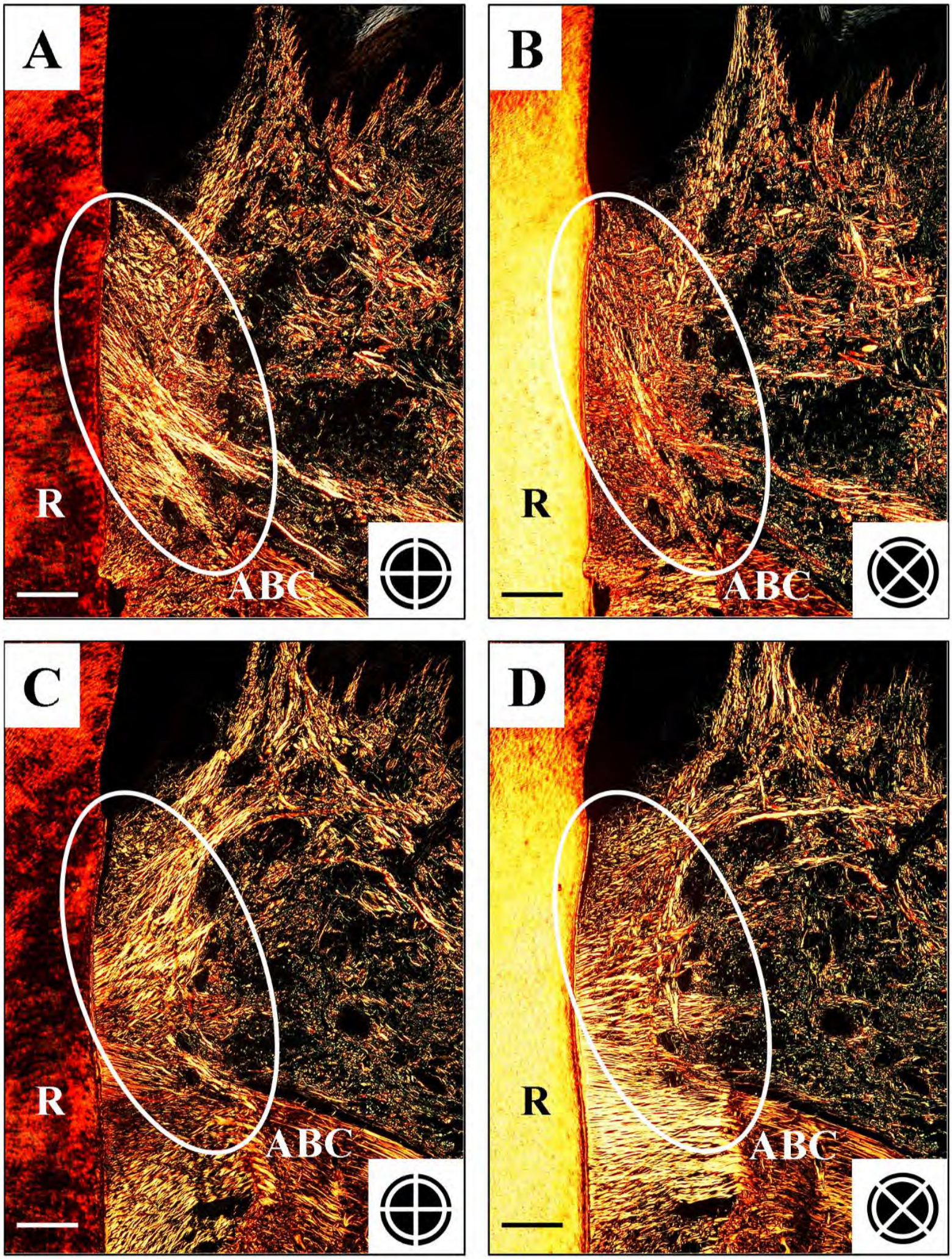
A
R
ABC
B
R
ABC
C
R
ABC
D
R
ABC